Sciences & Technologie **A** – **N°32** Décembre. (2010), pp. 35-41

CONJUGATE HEAT TRANSFER WITH VARIABLE FLUID PROPERTIES IN A HORIZONTAL ANNULUS

Reçu le 18/08/2009 – Accepté le 04/08/2010

Résumé

Dans le présent travail, on étudie numériquement le transfert de chaleur conjugué tridimensionnel dans un espace annulaire compris entre deux cylindriques concentriques horizontaux, dont le cylindre extérieur est soumis à une production d'énergie interne générée par effet Joule à travers son épaisseur tandis que celui intérieur est adiabatique. La convection thermique dans le domaine fluide est conjuguée à une conduction thermique dans le solide. Les propriétés physiques du fluide sont thermo-dépendantes et les pertes thermiques vers le milieu externe seront prises en compte. Les équations modélisantes de continuité, de mouvement et de l'énergie sont numériquement résolues par la méthode des volumes finis avec une discrétisation spatiotemporelle du second ordre. Les résultats obtenus montrent l'aspect tridimensionnel des champs thermiques et dynamiques avec des variations considérables de la viscosité et des variations modérées de la conductivité thermique du fluide. Comme prévu, le nombre de Nusselt de la convection mixte devient supérieur à celui de la convection forcée lorsque le nombre de Grashof est augmenté. Les résultats à l'interface solide-fluide du cylindre externe montrent clairement les variations azimutales et axiales du flux de chaleur local et du nombre de Nusselt local. Suite à ces résultats, nous avons essayé de modéliser le nombre de Nusselt moyen en fonction de nombre de Richardson. On trouve que la corrélation $Nu_i = 12.8678\ Ri^{0.1426}$ modélise les résultats avec les conditions et les paramètres de cette étude.

Mots-clés: Convection mixte laminaire, Cylindres concentriques, Transfert de chaleur conjugué, Simulation numérique.

S. TOUAHRI

T. BOUFENDI

Laboratoire de Physique Energétique
Département de Physique
Faculté des Sciences Exactes
Université Mentouri Constantine

Abstract

In the present work, we numerically study the three-dimensional conjugate heat transfer in an annular space between two horizontal concentric cylinders; the outer cylinder is subjected to an internal energy generated by Joule effect through its thickness while the inner is adiabatic. The thermal convection in the fluid domain is conjugated to the thermal conduction in the solid. The physical properties of the fluid are thermal dependant. The heat losses from the external outside pipe surface to the surrounding ambient are considered. The model equations of continuity, momenta and energy are numerically solved by a finite volume method with a second order spatiotemporal discretization. The obtained results show the three dimensional aspect of the thermal and dynamical fields with considerable variations of the viscosity and moderate variations of the fluid thermal conductivity. As expected, the mixed convection Nusselt number becomes more superior to that of the forced convection when the Grashof number is increased. At the solid-fluid interface, the results show clearly the azimuthal and axial variations of the local heat flux and the local Nusselt numbers. Following these results, we have tried modelling the average Nusselt number as a function of Richardson number. With the parameters used, the heat transfer is quantified by the correlation: $Nu_i = 12.8678\ Ri^{0.1426}$.

Keywords: Laminar Mixed Convection, Concentric Pipes, Conjugate Heat Transfer, Numerical simulation.

ملخص

في هذا العمل المنجز، ندرس رقميا التبادل الحراري الثلاثي الأبعاد بالحمل المختلط الرقائقي، ما بين قناتين أسطوانيتين أفقيتين متمركزتين ذوات سمك ضعيف، القناة الخارجية مسخنة بتيار كهربائي عابر خلال هذا السمك، في حين أن القناة الداخلية كظومة. الحمل المختلط في المائع مرافق للتوصيل الحراري في جدران القناة. الخواص الفيزيائية للمائع متعلقة بدرجة الحرارة، والضياع الحراري لجدار القناة الخارجية باتجاه الوسط الخارجي غير مهمل. معادلات الإنحفاظ النموذجية للكتلة، الحركة و الطاقة تحل عدديا بطريقة الحجوم المنتهية و باستعمال التقسيمات في الزمن و المكان من الدرجة الثانية. النتائج المتحصل عليها تبين المظهر الثلاثي الأبعاد للحرارة والحركة مع تغيرات معتبرة في اللزوجة وتغيرات أقل اعتبار في الناقلية الحرارية للمائع. عدد نوسالت (Nu) للحمل المختلط يصبح أكبر من عدد نوسالت للحمل القسري عند رفع عدد غراشوف. النتائج على السطح الفاصل بين المائع و جدار القناة الخارجية تبين بوضوح التغيرات الزاوية والمحورية للتدفق الحراري المحلي و عدد نوسالت المحلي. تبعا لهذه النتائج، حاولنا إيجاد علاقة تربط بين عدد نوسالت المتوسط و عدد ريشاردسون (Ri). نجد أن العلاقة $Nu_i = 12.8678\ Ri^{0.1426}$ هي التي تربط بين النتائج المتحصل عليها ومعطيات و شروط هذه الدراسة. المتحصل عليها ومعطيات و شروط هذه الدراسة..

الكلمات المفتاحيـــة: الحمل المختلط الرقائقي، قناتين متمركزتين، تبادل حراري مرافق، دراسة رقمية.

INTRODUCTION

Laminar mixed convection in a horizontal annulus has been studied by several workers. Nazrul et al. [1], studied numerically the heat transfer by laminar mixed convection in a concentric annulus, the inner cylinder subjected to constant heat flux, while the outer cylinder is adiabatic. The results obtained shows that the distribution of the velocity field and temperature are influenced by the transverse buoyancy force, for Ra = 10^5 and Ra = 10^7. Also, the Nusselt number at Z^*= 0.1 is greater than 30% and 110 %, respectively, compared to that of forced convection. Kotake et al [2], studied numerically the same problem. Two different boundary conditions: a constant heat flux, or a constant temperature of the outer wall. The numerical results of the average Nusselt number is in good agreement with other experimental results. Similar works has been done numerically by Kumar [3], Chung et *al.* [4] and Nouar [5], where the ratio D_O/D_I was considered. In the work of Habib et al [6], the inner cylinder is subjected to a non-uniform heat flux, while the outer surface is adiabatic. The change in axial Nusselt number in this work is in good agreement that of a numerical study under the same condition.

Experimentally, the heat transfer by mixed convection in annulus was studied by Mohammed et al. [7] with two concentric cylinders made of steel, $D_O/D_I = 2$, the inner tube subjected to a constant heat flux, the outer tube is adiabatic, the Reynolds number is varied from 200 to 1000, while the Grashof number variation is between $6.2\cdot10^5$ and $1.2\cdot10^7$. The results show that the average Nusselt number can be linked with different dimensionless numbers by the correlation: $Nu_A = 2.964\,(Gr\cdot \mathrm{Pr}/\mathrm{Re})^{0.0326}$

In this work, we studied numerically the heat transfer by mixed convection in an annulus between two concentric cylinders, the physical properties of the fluid are thermo-dependent and the heat losses with the external environment are considered. The objective of our study is the exploration of the dynamical and thermal fields for the complete system fluid-solid and the obtaining a correlation of the average Nusselt numbers and Richardson.

THE MATHEMATICAL MODEL

Figure1 illustrates the problem geometry. We consider two long horizontal concentric pipes having a length L = 1 m. The internal pipe with an inside diameter D_{1i} = 0.46 cm and an external diameter D_{1o} = 0.5 cm, the external pipe with an inside diameter D_{2i} = 0.96 cm and an external diameter D_{2o} = 1cm. The hydraulic diameter $D_h=D_{2i}-D_{1o}$=0.46cm.The pipes are made of Inconel having a thermal conductivity K_s = 20 W/m°K. The passing of an electrical current along the thickness of the external pipe produced a heat generation by the Joule effect. The considered electrical intensities values are: I =40, 45, 50, 55, 60 and 65 Amperes.

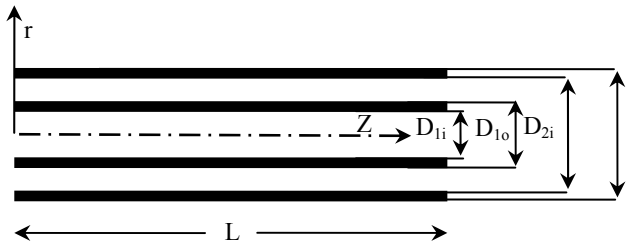

Figure 1. Geometry of the problem

This generated heat is transferred to laminar incompressible flow of distilled water with an average entrance velocity V_0 equal to 9.88 10^{-2} m/s. The inside surface of the internal pipe is insulated and at the outer surface of the external pipe, the heat losses by radiation and natural convection to the surrounding air are taken into account. At the annulus entrance, we have a uniform temperature equal to 288°K, the Reynolds number is equal to 399.02 and the Prandtl number is equal to 8.082. The Grashof numbers corresponding to the electrical intensities are: 4848, 6135, 7575, 9165, 10908, and 12801, respectively. The fluid viscosity and thermal conductivity variation with temperature are represented by the functions $\mu^*(T^*)$ and $K^*(T^*)$ obtained by smooth fittings of the tabulated values cited by Baehr and Stephan [8].

The combined heat transfer in the solid and fluid domains is a conjugate heat transfer problem. The physical principles involved in this problem are well modelled by the following non dimensional conservation partial differential equations with their initial and boundary conditions:

Dimensionless Modelling Equations

In this paper the star superscript (*) make reference to a dimensionless quantity.

At $t^* = 0$, $\quad V_r^* = V_\theta^* = V_z^* = T^* = 0$ (1)

V_r^*, V_θ^*, V_z^* are the radial, angular and axial velocity component = (V_r/V_0), (V_θ/V_0) , (V_z/V_0), the temperature $T^* = (T-T_0)/(G\,D_h^2/K_s)$ and the time $t^* = (V_0\,t/D_h)$

At $t^* > 0$,

Mass conservation equation

$$\frac{1}{r^*}\frac{\partial}{\partial r^*}\left(r^*\,V_r^*\right)+\frac{1}{r^*}\frac{\partial V_\theta^*}{\partial \theta}+\frac{\partial V_z^*}{\partial z^*} = 0 \qquad (2)$$

r^*, θ, z^* are the radial, angular and axial coordinates.

Radial momentum conservation equation

$$\frac{\partial V_r^*}{\partial t^*}+\frac{1}{r^*}\frac{\partial}{\partial r^*}\left(r^* V_r^* V_r^*\right)+\frac{1}{r^*}\frac{\partial}{\partial \theta}\left(V_\theta^* V_r^*\right)+$$
$$\frac{\partial}{\partial z^*}\left(V_z^* V_r^*\right)-\frac{V_\theta^{*2}}{r^*}=-\frac{\partial P^*}{\partial r^*}+\frac{Gr_0^*}{\mathrm{Re}_0^2}\cos\theta\ T^*+$$
$$\frac{1}{\mathrm{Re}_0}\left[\frac{1}{r^*}\frac{\partial}{\partial r^*}\left(r^*\tau_{rr}^*\right)+\frac{1}{r^*}\frac{\partial}{\partial\theta}\left(\tau_{r\theta}^*\right)-\frac{\tau_{\theta\theta}^*}{r^*}+\frac{\partial}{\partial z^*}\left(\tau_{rz}^*\right)\right] \quad (3)$$

Where the Reynolds number Re is $\left(V_0 D_h/\nu_0\right)$ and the Grashof number is $\mathrm{Gr}^* = g\beta GD_i^5/K_s\nu^2$.

Angular momentum conservation equation

$$\frac{\partial V_\theta^*}{\partial t^*}+\frac{1}{r^*}\frac{\partial}{\partial r^*}\left(r^* V_r^* V_\theta^*\right)+\frac{1}{r^*}\frac{\partial}{\partial\theta}\left(V_\theta^* V_\theta^*\right)+$$
$$\frac{\partial}{\partial z^*}\left(V_z^* V_\theta^*\right)+\frac{V_r^* V_\theta^*}{r^*}=-\frac{1}{r^*}\frac{\partial P^*}{\partial\theta}-$$
$$\frac{Gr_0^*}{\mathrm{Re}_0^2}\sin\theta\ T^*+\frac{1}{\mathrm{Re}_0}\left[\begin{array}{l}\frac{1}{r^{*2}}\frac{\partial}{\partial r^*}\left(r^{*2}\tau_{\theta r}^*\right)+\\ \frac{1}{r^*}\frac{\partial}{\partial\theta}\left(\tau_{\theta\theta}^*\right)+\frac{\partial}{\partial z^*}\left(\tau_{\theta z}^*\right)\end{array}\right] \quad (4)$$

P^* is the pressure, $\left(P-P_0\right)/\rho_0 V_0^2$.

Axial momentum conservation equation

$$\frac{\partial V_z^*}{\partial t^*}+\frac{1}{r^*}\frac{\partial}{\partial r^*}\left(r^* V_r^* V_z^*\right)+\frac{1}{r^*}\frac{\partial}{\partial\theta}\left(V_\theta^* V_z^*\right)+$$
$$\frac{\partial}{\partial z^*}\left(V_z^* V_z^*\right)=-\frac{\partial P^*}{\partial z^*}+$$
$$\frac{1}{\mathrm{Re}_0}\left[\frac{1}{r^*}\frac{\partial}{\partial r^*}\left(r^*\tau_{rz}^*\right)+\frac{1}{r^*}\frac{\partial}{\partial\theta}\left(\tau_{\theta z}^*\right)+\frac{\partial}{\partial z^*}\left(\tau_{zz}^*\right)\right] \quad (5)$$

Energy conservation equation

$$\frac{\partial T^*}{\partial t^*}+\frac{1}{r^*}\frac{\partial}{\partial r^*}\left(r^* V_r^* T^*\right)+\frac{1}{r^*}\frac{\partial}{\partial\theta}\left(V_\theta^* T^*\right)+$$
$$\frac{\partial}{\partial z^*}\left(V_z^* T^*\right)=G^*-$$
$$\frac{1}{\mathrm{Re}_0\ \mathrm{Pr}_0}\left[\begin{array}{l}\frac{1}{r^*}\frac{\partial}{\partial r^*}\left(r^* q_r^*\right)+\\ \frac{1}{r^*}\frac{\partial}{\partial\theta}\left(q_\theta^*\right)+\frac{\partial}{\partial z^*}\left(q_z^*\right)\end{array}\right] \quad (6)$$

Where $G^* = \begin{cases} K_S^*/\left(\mathrm{Re}_0\,\mathrm{Pr}_0\right) & \text{in the solid} \\ 0 & \text{in the fluid}\end{cases}$

G^* is the heat generation $= \left(K_S^*/\mathrm{Re}_0\,\mathrm{Pr}_0\right)$.

The viscous stress tensor components are:

$$\tau_{rr}^* = 2\mu^*\frac{\partial V_r^*}{\partial r^*}, \qquad \tau_{r\theta}^* = \tau_{\theta r}^* = \mu^*\left[r^*\frac{\partial}{\partial r^*}\left(\frac{V_\theta^*}{r^*}\right)+\frac{1}{r^*}\frac{\partial V_r^*}{\partial\theta}\right]$$
$$\tau_{\theta\theta}^* = 2\mu^*\left[\frac{1}{r^*}\frac{\partial V_\theta^*}{\partial\theta}+\frac{V_r^*}{r^*}\right], \qquad \tau_{\theta z}^* = \tau_{z\theta}^* = \mu^*\left[\frac{\partial V_\theta^*}{\partial z^*}+\frac{1}{r^*}\frac{\partial V_z^*}{\partial\theta}\right] \quad (7)$$
$$\tau_{zz}^* = 2\mu^*\frac{\partial V_z^*}{\partial z^*}, \qquad \tau_{zr}^* = \tau_{rz}^* = \mu^*\left[\frac{\partial V_z^*}{\partial r^*}+\frac{1}{r^*}\frac{\partial V_r^*}{\partial z^*}\right]$$

The heat fluxes are:

$$q_r^* = -K^*\frac{\partial T^*}{\partial r^*}, \quad q_\theta^* = -\frac{K^*}{r^*}\frac{\partial T^*}{\partial\theta^*} \text{ and } q_Z^* = -K^*\frac{\partial T^*}{\partial z^*} \quad (8)$$

Boundary Conditions

At the annulus entrance : $Z^*=0$

* In the fluid domain:

$0.5435 \le r^* \le 1.0435$ *and* $0 \le \theta \le 2\pi$

$$V_r^* = V_\theta^* = T^* = 0, V_z^* = 1 \quad (9)$$

* In the solid domain:

$0.5 \le r^* \le 0.5435$ *or* $1.0435 \le r^* \le 1.0870$ *and* $0 \le \theta \le 2\pi$

$$V_r^* = V_\theta^* = V_z^* = T^* = 0 \quad (10)$$

At the annulus exit : $Z^*=217.39$

* In the fluid domain:

$0.5435 \le r^* \le 1.0435$ *and* $0 \le \theta \le 2\pi$

$$\frac{\partial V_r^*}{\partial z^*} = \frac{\partial V_\theta^*}{\partial z^*} = \frac{\partial V_z^*}{\partial z^*} = \frac{\partial}{\partial z^*}\left(K^*\frac{\partial T^*}{\partial z^*}\right) = 0 \quad (11)$$

* In the solid domain:

$0.5 \le r^* \le 0.5435$ *or* $1.0435 \le r^* \le 1.0870$ *and* $0 \le \theta \le 2\pi$

$$V_r^* = V_\theta^* = V_z^* = \frac{\partial}{\partial z^*}\left(K^*\frac{\partial T^*}{\partial z^*}\right) = 0 \quad (12)$$

At the inside wall of internal pipe: $r^*=0.5$

$$V_r^* = V_\theta^* = V_z^* = 0 \text{ and } \frac{\partial T^*}{\partial r^*} = 0 \quad (13)$$

At the outer wall of external pipe: $r^*=1.0870$

$$\begin{cases} V_r^* = V_\theta^* = V_z^* = 0 \\ -K^*\dfrac{\partial T^*}{\partial r^*} = \dfrac{\left(h_r + h_c\right)D_i}{K_0}T^* \end{cases} \quad (14)$$

$$h_r = \varepsilon\,\sigma\left(T^2 + T_\infty^2\right)\left(T + T_\infty\right) \quad (15)$$

h_r : radiative heat transfer coefficient

h_c : convective heat transfer coefficient

The emissivity of the outer wall ε is arbitrarily chosen to 0.9 while h_c is derived from the correlation of Churchill and Chu [9] valid for all Pr and for Rayleigh numbers in the range $10^{-6} \le \mathrm{Ra} \le 10^9$.

$$Nu = \left[h_c D_i / K_{air}\right] = \left[0.6 + \left(0.387\,Ra^{1/6}/\left(1+\left(0.559/\mathrm{Pr}_{air}\right)^{9/16}\right)^{8/27}\right)\right]^2 \quad (16)$$

The Nusselt number

At the solid-fluid interface (r^*=1.0435) the local Nusselt number is defined as:

$$Nu\left(\theta, Z^*\right) = \frac{h\left(\theta, Z^*\right)D}{k} = \frac{1}{\left[T^*\left(r^*,\ \theta,\ z^*\right) - T_m^*\left(z^*\right)\right]} \quad (17)$$

$Nu\left(\theta, Z^*\right)$: Local Nusselt number.

The axial Nusselt $Nu\left(Z^*\right)$ number is defined as:

$$Nu\left(z^*\right) = \frac{1}{2\pi}\int_0^{2\pi} Nu\left(\theta, z^*\right)d\theta \quad (18)$$

The average Nusselt number for the whole solid-fluid interface is defined as:

$$Nu_A = \frac{1}{(2\pi)(217.39)} \int_0^{2\pi} \int_0^{104.17} Nu(\theta, z^*)\, dz^*\, d\theta \qquad (19)$$

Nu_A is the average Nusselt number.

THE NUMERICAL RESOLUTION

For the numerical solution of modelling equations, we used the finite volume method well described by Patankar [10]. The using of this method involves the discretization of the physical domain into a discrete domain constituted of finite volumes where the modelling equations are discretized in a typical volume. We used a temporal discretization with a truncation error of $(\Delta t^*)^2$ order. The mesh used contains 26×44×162 points in the radial, azimuthal and axial directions. The considered time step is $\Delta t^* = 5 \cdot 10^{-4}$. The accuracy of the results of our numerical code has been tested by the comparison of our results with those of Carlo and Guidice [11] who studied numerically the conjugate mixed convection heat transfer in annulus with finite element method. The controlling parameters of the problem are: Re = 1000, Pr = 0.7, Gr^* = 10^6, $R_2/R_1 = 2$. In **Figure 2** we illustrate the axial evolution of the circumferentially averaged Nusselt number. It is seen that there is a good agreement between our results and theirs.

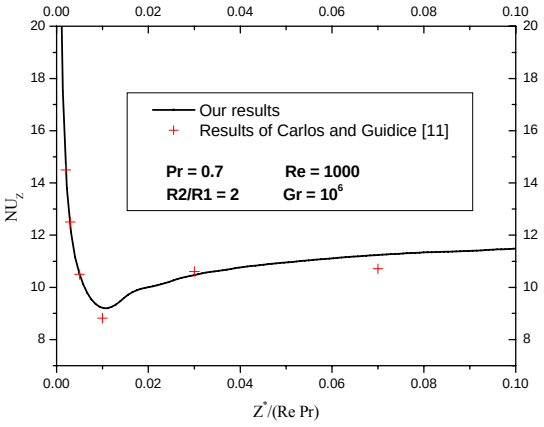

Figure 2. Axial evolution of the circumferentially mean local axial Nusselt number; a comparison with the results of Carlo and Guidice [11].

RESULTS AND DISCUSSIONS

Development of the secondary flow

The obtained flow for the considered cases is characterized by a main flow in the axial direction and a secondary flow in $(\overrightarrow{r^*}, \theta)$ plan. Qualitatively we note the similarity of results for the six study cases. Quantitatively, the effect of mixed convection becomes increasingly important with the increase of volumetric heating. This is why we have chosen to present the corresponding figures for the higher volumetric heating case, Gr *= 12801. In **Figure 3**, we present the secondary flow at the annulus exit (Z^*=217.39).

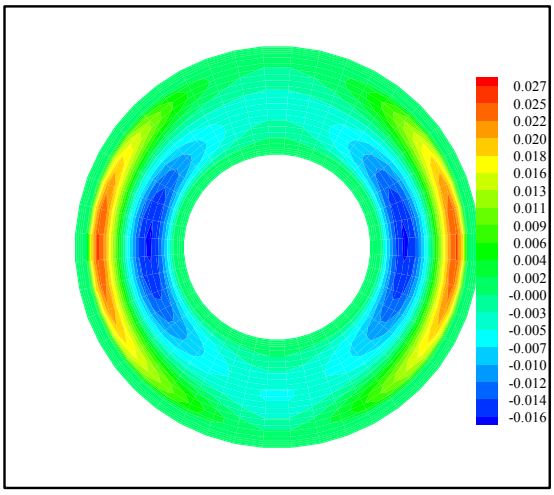

Figure 3 Secondary flow at the exit of the annulus for Gr^*=12801

The transverse movement is explained as follows: the hot fluid moves along the hot wall from the bottom of the outer tube $(\theta = \pi)$ upwards $(\theta = 0)$ and moves down from the top to the bottom along the inner tube. The vertical plane passing through the angles $(\theta = 0)$ and $(\theta = \pi)$ is a plane of symmetry. The transverse flow in the $(\overrightarrow{r^*}, \theta)$ plane is represented by two similar but counter rotating cells. We noticed that the center of the rotating cells moves downward continuously along the axial direction.

D Development of the Axial Flow

At the entrance, the axial flow is axisymmetric, after this latter is influenced by the transverse movement of the fluid. The maximum axial velocity is all the time at the top of the annulus because the fluid viscosity decreased from bottom to top. In **Figure 4**, we present the axial flow distribution at the exit of the annulus.

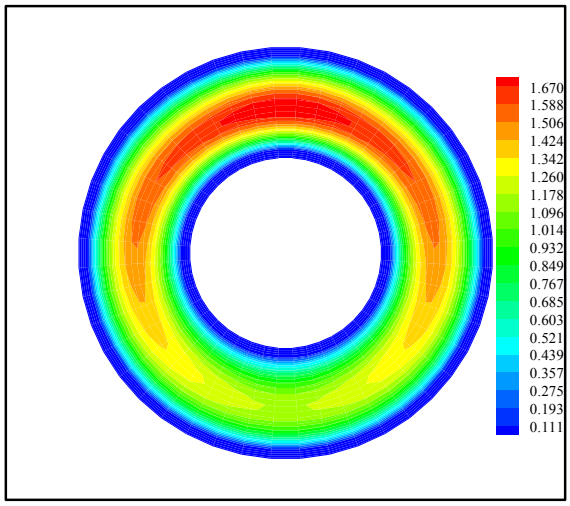

Figure 4 Axial velocity profiles at the exit of the annulus for Gr^*=12801

all the time located at $r^* = 1.0435$ and $\theta = 0$ (top of solid-fluid interface), because the hot fluid is driven by the secondary motion towards the top of the annulus. The minimum temperature is within the core fluid, in the lower part of the annulus at $\theta = \pi$. In **Figure 5**, we present the polar temperature distribution at the exit of the annulus for Gr^*=12801. To see the effect of the secondary flow on the temperature of external cylinder, we propose in **Figure 6** a comparison of the temperatures between the top and the bottom of the inner wall of the external pipe. At the entrance, the temperature difference between the top and the bottom of the outer cylinder is zero while this difference becomes very important at the exit and equal to 25.97 ° C. The large variation in physical properties with temperature is shown in **Figure 7**. The dynamic viscosity in the annulus decreases from 1.02 at the entrance to 0.23 at the exit. At given section, the minimum of the dynamic viscosity is always at $r^* = 1.0435$ and $\theta = 0$ because the maximum of temperature is in this position.

Development of the temperature field

In the reference case (forced convection), the distribution of the fluid temperature in the absence of transverse motion is axisymmetric. For a given section, the isotherms are concentric circles with a maximum temperature on the inner wall of the external cylinder and a minimum temperature on the outer wall of the internal cylinder. In the presence of volumetric heating, a transverse flow exists and thus changes the axisymmetric distribution of fluid and pipe wall temperature and gives it an angular variation, this variation explained as follows: the hot fluid near the hot pipe wall moves upwards under the buoyancy force effect, the relatively cold fluid descends down near the internal pipe.

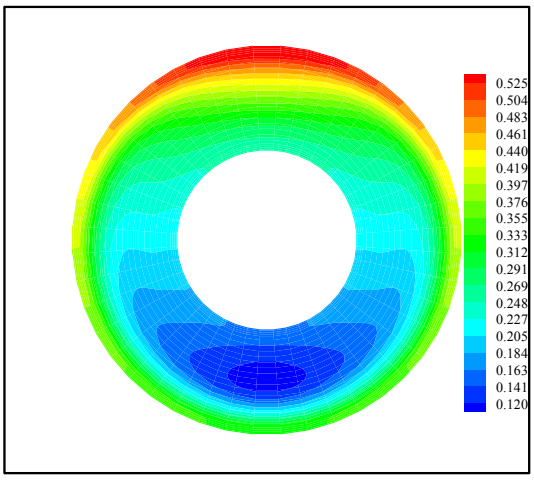

Figure 5. The isotherms at the exit of the annulus for Gr^*=12801

This movement of the secondary flow is the cause of the azimuthally temperature variation. The obtained results show that at given section, the maximum temperature T^* is

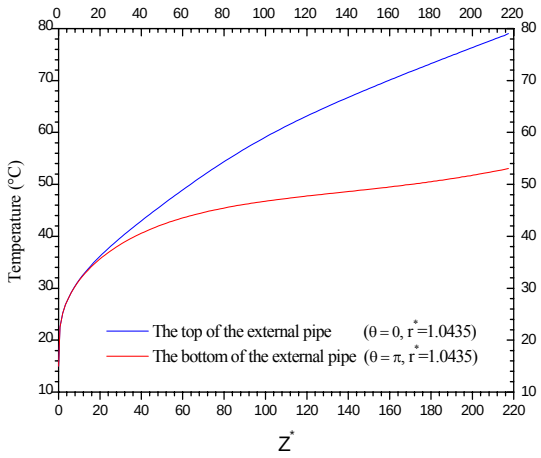

Figure 6. The inner wall temperature of the external pipe

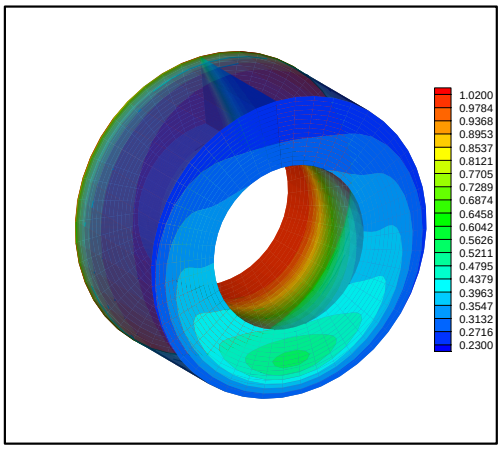

Figure 7. The dimensionless dynamic viscosity variation for Gr^*=12801

The Nusselt numbers

The phenomenon of heat transfer has been characterized in terms of circumferentially Nusselt numbers calculated at the inner wall of the external pipe, which is obtained by (17). The variation of the local Nusselt number at the solid-fluid interface is presented in Fig. 8 for Gr^*=12801. From the entrance to the exit, we notice the large axial and angular variations of local Nusselt numbers; it takes a minimum value equal to 4.45 at $\theta = 0$ and a maximum value equal to 20.94 at $\theta = \pi$.

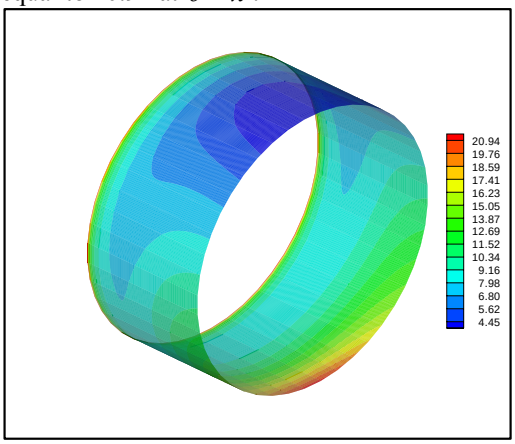

Figure 8. The local Nusselt number variation for Gr^* =12801.

The axial Nusselt number $Nu(z^*)$ is obtained by (18). **Figure 9** shows the axial variation of Nusselt number for the seven studied cases. At the zone of entrance, the axial Nusselt number decreases rapidly for all studied cases. After, it increases and takes maximum value at the exit of annulus equal to: 7.75, 8.34, 8.96, 9.60, 10.27 and 10.95 for Gr^* = 4848, 6135, 7575, 9165, 10908, and 12801 respectively. The axial Nusselt numbers increases with the increase of volumetric heating.

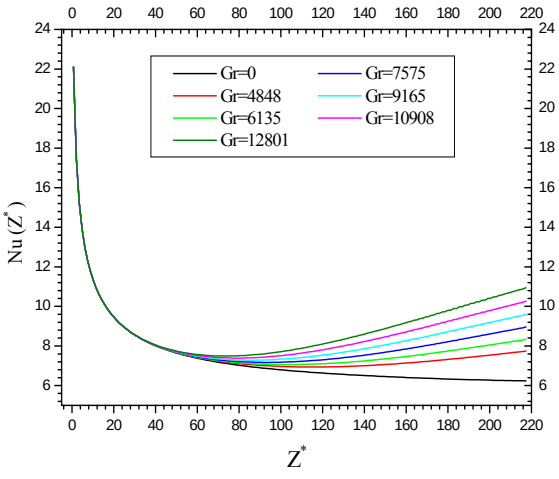

Figure 9. The axial variation of the Nusselt number for different Grashof numbers

The average Nusselt number Nu_A is obtained by (19). In Table 1 we present the average Nusselt numbers of all studied cases.

Table 1 Average Nusselt Numbers

Gr*	4848	6135	7575	9165	10908	12801
Ri	0.030	0.039	0.048	0.058	0.069	0.080
Nu_A	7.880	8.071	8.287	8.522	8.779	9.050

The results obtained allowed us to model the average Nusselt number of the mixed convection in function of Richardson number, we found that the results with the parameters used are correlated with the correlation:

$$Nu_A = 12.8678\ Ri^{0.1426} \quad (20)$$

CONCLUSION

This study considers the numerical simulation of the three dimensional mixed convection heat transfer horizontal annulus, the external pipe is heated by an electrical intensity passing through its small thickness and the internal pipe is insulated. The obtained results show that:

* The dynamic and thermal fields for mixed convection are qualitatively and quantitatively different from those of forced convection.
* Although the volumetric heat input in the solid thickness is constant, the heat flux at the solid-fluid interface is not constant: it varies with θ and z^*, which is a characteristic of the considered mixed convection.
* The azimuthally variation of temperature at a given section is important; this phenomenon is demonstrated by the circumferential temperature variation of the wall. There is a large temperature wall difference between top and bottom of the external pipe.
* The physical properties are thermo-dependent (dynamic viscosity varies from 1.14 10^{-6} at the entrance to 0.27 10^{-6} m^2/s at the exit).
* For the forced convection, the average Nusselt number is 7.45. Thus, for the mixed convection, the parameters used are well correlated with the correlation:

$$Nu_A = 12.8678\ Ri^{0.1426}.$$

REFERENCES

[1] Islam. N, U. N. Gaitonde. U. and Sharma. G. K, "Mixed convection heat transfer in the entrance region of horizontal annuli", *Int. J. Heat Mass Transfer*, vol. 44, (2001), pp. 2107-2120.

[2] Kotake. S, Hattori. N, "Combined forced and free convection heat transfer for fully-developed laminar flow in horizontal annuli", *Int. J. Heat Mass Transfer*, vol. 28, (1985), pp. 2113-2120.

[3] Kumar. R, "Study of natural convection in horizontal annuli", *Int. J. Heat Mass Transfer*, vol. 31, (1988), pp. 1137-1148.

[4] Chung. S. Y, Rhee. G. H, and Sung. H. J, "Direct Numerical Simulation of Concentric Annular Pipe Flow"

Part I: Flow Field, Int. J. Heat Fluid Flow, vol. 23, (2002), pp. 426-440.
[5] NOUAR. C, "Numerical solution for laminar mixed convection in a horizontal annular duct: temperature-dependent viscosity effect", *Int. J. Numer. Meth. Fluids* Vol. 29, (1999), pp. 849–864.
[6] Habib. M. A, Negm. A. A, "Laminar mixed convection in horizontal concentric annuli with non-uniform circumferential heating", *Int. J. Heat Fluid Flow*, Vol. 37, (2001), pp. 427-435.
[7] Mohammed H. A, Campo A and Saidur. R, "Experimental study of forced and free convective heat transfer in the thermal entry region of horizontal concentric annuli", *International Communications in Heat and Mass Transfer*, Vol. 37, (2010), pp. 739–747.
[8] H.D. Baehr and K. Stephan, *Heat and Mass Transfer,* Transl, by N. JanePark, p. 619, pringer-Verlag, Berlin: (1998).
[9] Churchill. S. W, Chu. H. S, "Correlating Equation for Laminar and Turbulent Free Convection from a Horizontal Cylinder", *International Journal of Heat and Mass Transfer,* Vol 18, (1975), pp. 1049-1053
[10] Patankar. S. V, *Numerical Heat Transfer and Fluid Flow*, McGraw-Hill, New-York: (1980).
[11] Carlo. N, Guidice. S. D, "Finite element analysis of laminar mixed convection in the entrance region of horizontal annular ducts", *Numer. Heat Transfer*, Part A, 29, (1996), pp 313-330.